Physica B 456 (2015) 197–205

Contents lists available at ScienceDirect

Physica B

journal homepage: www.elsevier.com/locate/physb

Effect of substrates on the growth of α-MoO_3 nanostructures via plasma assisted sublimation process

Rabindar K. Sharma *, G.B. Reddy

Thin film laboratory, Department of Physics, Indian Institute of Technology Delhi, New Delhi 110016, India

ARTICLE INFO

Article history:
Received 15 April 2014
Received in revised form
23 August 2014
Accepted 27 August 2014
Available online 4 September 2014

Keywords:
Molybdenum oxide
Substrate effect
Plasma assisted sublimation process (PASP)

ABSTRACT

In this communication, we have investigated the substrate effect on the growth of MoO_3 nanostructured thin films prepared by plasma assisted sublimation process (PASP). Three different substrates viz. ITO glass, Ni/Si [100], and Ni/glass are used in deposition process. The surface analysis endorsed that Ni/Si and Ni/glass substrates are most favorable for the uniform growth of vertically aligned MoO_3 nanoplates (NP_s) and nanoflakes (NF_s) of well controlled features with very high aspect ratio (height/thickness) >30, whereas nanostructure formed on ITO/glass substrate is improper (in terms of features and alignment). The X-ray diffractograms divulge that MoO_3 films deposited on all substrates exhibit pure orthorhombic phase with preferential crystallographic orientation along [110] direction particularly in case of Ni/Si and Ni/glass substrates. Atomic force microscopic analysis reveals that the average substrates roughness enhanced in presence of pre-deposited layer and monitor the growth of nanostructures. High resolution transmission electron microscopic analysis with selected area diffraction pattern confirmed that both the MoO_3 NP_s and NF_s are single crystalline in nature. The Raman and IR spectrum of all films further endorse the presence of single orthorhombic phase in accordance with the XRD results and also confirm the effect of nanosize on the vibrational properties.

1. Introduction

The remarkable research interest has been focused on quasi-one dimensional materials due to their unique electrical, optical, and mechanical properties, and as a result, they have promising applications in nanodevices. The impression of dimensionality and geometry on nanomaterials has been extensively studied to meet the demand of miniaturization and better performance for various applications. Particularly, nanostructured metal oxide with reduced dimensions and high surface area are increasing attraction owing to their excellent optical, electrical, magnetic, and ionic transport properties, fabrication of such crystalline metal oxide is very popular during the past decade [1]. Molybdenum trioxide (MoO_3) as one of the well-known n-type semiconductor is attractive due to its multifaceted structural and functional properties. It is attractive because of its various potential applications in many fields, such as photochromic devices, [2] electrochromic devices, [3] gas sensors, [4] catalysts, [5] generating enhanced electric field emission, [6] and in Li^+ ion batteries [7]. Generally, MoO_3 is existed mainly in three different crystalline polymorphs, orthorhombic (α-MoO_3), monoclinic (β-MoO_3), and hexagonal (h-MoO_3). Among them α-MoO_3 is a thermodynamically stable phase with layered structure and most studied one. The structure of bulk .α-MoO_3 has been theoretically demonstrated as possessing a crystallographic anisotropic structure in many reports. Its anisotropy is mainly the reflection of distorted MoO_6 octahedra shearing corners in the direction of [100] (*a*-axis) and the zigzag edges in the direction of [001] (*c*-axis) to form a single layer. Two single layers stacked together by Vander Waals force along the *b*-axis to construct bilayer. This peculiar structural behavior makes MoO_3 one of the pronounced candidates to form the nanostructures with very high surface to volume ratio [8]. For nanostructures particularly in case of nanoplates and nanoflakes, their single crystalline nature and sufficiently large aspect ratio make them ideal candidates for probing size and dimensionality .dependent physical and chemical phenomenon as well as in nanodevices applications. For these applications, aspect and surface to volume ratio are found to be most crucial factors that affect the efficient parameters, especially when the dimensions of material are reduced to the order of nanoscale. Depending on the process, MoO_3 have synthesized in the different nano- or micro-scale surface morphologies that includes wires, rods, belts, flakes, and

* Corresponding author.
E-mail address: rkrksharma6@gmail.com (R.K. Sharma).

http://dx.doi.org/10.1016/j.physb.2014.08.040
0921-4526/

plates. The number of different techniques have been reported for the deposition of MoO_3 nanostructured thin films including pulse electron beam deposition, [6] thermal evaporation, [9] flame synthesis, [10] r.f magnetron sputtering, [11] and sol–gel [12]. Liu et al. [8] have achieved the α-MoO_3 nanorods on Si substrate [010] by pulse electron beam deposition. Cai et al. [10] reported the morphologically-controlled flame synthesis of flower like α-MoO_3 nanobelts arrays on silicon substrates. Zhou et al. [13] proposed the well aligned MoO_3 nanowires synthesized by thermal evaporation process followed by oxidation and used silicon [100] as a substrate. RF magnetron method was used by Rao et al. to yield the MoO_3 films and study their optical and infrared properties [11]. Hsu et al. attempted to grow nanocrystalline MoO_3 thin films on ITO coated glass using sol–gel spin coating method [14]. Yan et al. [15] presented the growth of α-MoO_3 nanoflakes (NFs) on Au/Si substrate at temperature 450 °C by a modified hot plate method. But in this case, the number density (number of NF_s per unit area) is relatively small. Khademi et al. [16] also have been yielded MoO_3 nanostars with improved number/coverage density using thermal evaporation at extremely high growth temperature nearly 1300 °C. Comini et al. [17] have grown nanorods on alumina substrate via. IR-irradiation heating a Mo foil directly in air. In addition to the listed above, many research groups have exploited several synthesis routes either individual or followed by some post deposition treatments to form the variety of nanostructures on different kinds of substrates. Even though these routes are effective from the growth point of view, but have some limitations. .Many of them required templates/surfactants and very high order of vacuum as well as temperature, whereas the chemical routes are relatively more complex, produce more or less contaminations and toxic gases as well.

In this work, we report plasma assisted sublimation process (PASP) accompanied with the joule heating of Mo-strip is exploited to grow the MoO_3 nanostructures on different kind of substrates and discussed the influence of substrate nature on the growth of nanostructures briefly. There are various advantages of PASP over the other reported deposition routes. In this deposition process, oxygen plasma is exploited as a growth monitoring parameter. The uniqueness of PASP is that the oxidation of Mo metal is taking place in-situ the oxide volatilization at relatively lesser temperature in oxygen plasma than normal oxygen ambient. The plasma ambience is not only facilitates oxidation at much lower temperature but also distribute the MoO_3 molecules on large area of substrates in a homogeneous fashion, attributed to controlled and uniform growth with very high coverage density. Three different substrates viz. ITO/glass, Ni/Si [100], and Ni/glass substrates are used in the deposition process under the exactly same processing parameters. The comparative studies concerning morphological, structural, and optical properties of nanostructures grown on the variety of substrates are investigated systematically. According to the AFM observations, the degree of average surface roughness of substrates is enhanced in presence of pre-deposited layers and greatly influenced the number of nanostructural units like (nanoplates/nanoflakes) per unit area. The SEM analysis shows that nickel coated silicon and glass substrates are most appropriate for the vertically aligned growth of MoO_3 2D nanostructures (i.e. NP_s and NF_s) with very high aspect ratio. All MoO_3 films on different substrates are polycrystalline in nature and having pure orthorhombic crystalline phase. Both the NP_s and NF_s grown on the Ni coated silicon and Ni coated glass, respectively are preferentially oriented along the [110] crystallographic direction whilst in case of ITO/glass the structures grown randomly in all the possible crystal directions. The vibrational study of all samples are carried out by using Raman and infra-red (IR) spectroscopy, which further assured the existence of single orthorhombic phase and endorse the nanosize effect on the vibrational properties as well. All the observed results are well in consonance with each other.

2. Experimental

Molybdenum oxide nanostructured thin films are deposited on three substrates: ITO/glass, Ni/Si [100], and Ni/bare glass substrates the by a remarkably effective approach called PASP. First the nickel film of thickness more than 100 nm is deposited on Si [100] and glass substrates by thermally evaporating (99.99% Aldrich) pure nickel powder at the base vacuum of 7.5×10^{-6} Torr. Then, substrates are mounted individually in the center of Mo-strip (act as a sublimation source) and gradually increasing the sublimation source temperature up to 500 °C from rate ~70 °C/min by suitably adjusting the current passed through the Mo-strip. The substrate as well as source temperature is measured using thermocouple arrangement. The observed temperature gradient between glass substrate and Mo-strip was almost 50 °C, whereas negligible for silicon substrate. The ratio of substrate area (20×15) mm^2 to that of Mo-strip (8×3) cm^2 is maintained nearly 1/8 for all substrates in order to obtain uniform deposition. The heated Mo-strip along with substrate was placed in oxygen plasma. The plasma parameters viz. plasma voltage, electrode separation and oxygen partial pressure are maintained at their optimum values 2500 V, 7.5 cm, and 7.5×10^{-2} Torr, respectively during growth. The film depositions on all substrates are executed for 1/2 h after that samples are allowed to cool naturally at room temperature. The MoO_3 films deposited on ITO/glass, Ni/Si [100], and Ni/bare glass substrates are abbreviated as S1, S2, and S3, respectively. The average surface roughness of all substrates is measured by atomic force microscope of model (Nanoscope IIIa) operating in tapping mode. The surface microstructures of deposited nanostructured thin films on the considered substrates are studied with scanning electron microscope ZEISS-EVO series scanning electron microscope model EVO-50. Structural analysis of samples are carried out by using Philips X-Ray diffractometer using Cu-K_α radiation ($\lambda \sim 1.54$ A) with glancing angle kept constant at 1°. Vibrational study of MoO_3 films was carried out by micro-Raman spectroscopy of Renishaw-inVia (excited with a Ar^+ line at 514.5 nm) and Perkin Elmer (Spectrum BX2) FTIR in the spectral range from 200–1050 cm^{-1} and 400–2000 cm^{-1}, respectively. Transmission electron microscopy (TEM) studies of samples are carried out by Philips Model CM12 operated at 120 kV with the selected area electron diffraction (SAED) analysis. Further to study the crystalline properties in more accuracy, HRTEM characterization of samples is performed at comparatively higher magnifications of samples S2 and S3 individually. All measurements are performed at room temperature.

3. Results and discussions

3.1. XRD studies

In order to determine the overall phase composition and purity of MoO_3 thin films as well as the crystalline behavior of Ni film, X-ray diffractograms (XRD) are recorded. Fig. 1 depicts the XRD of MoO_3 films deposited on S1–S3, whereas Fig. 2 shows the XRD of annealed ITO/Ni films at 500 °C in vacuum of the order of 7.5×10^{-5} Torr on all the assumed substrates before MoO_3 deposition. Fig. 1 shows very sharp diffraction peaks in the diffractograms of samples S1–S3 are endorsed the polycrystalline nature of films and evident the existence of nanostructures as well. All the observed diffraction peaks arewell indexed and confirm the formation of orthorhombic crystal .structures of MoO_3 thin films with the lattice constants of $a = 3.964$ Å $b = 13.842$ Å and $c = 3.692$ Å,

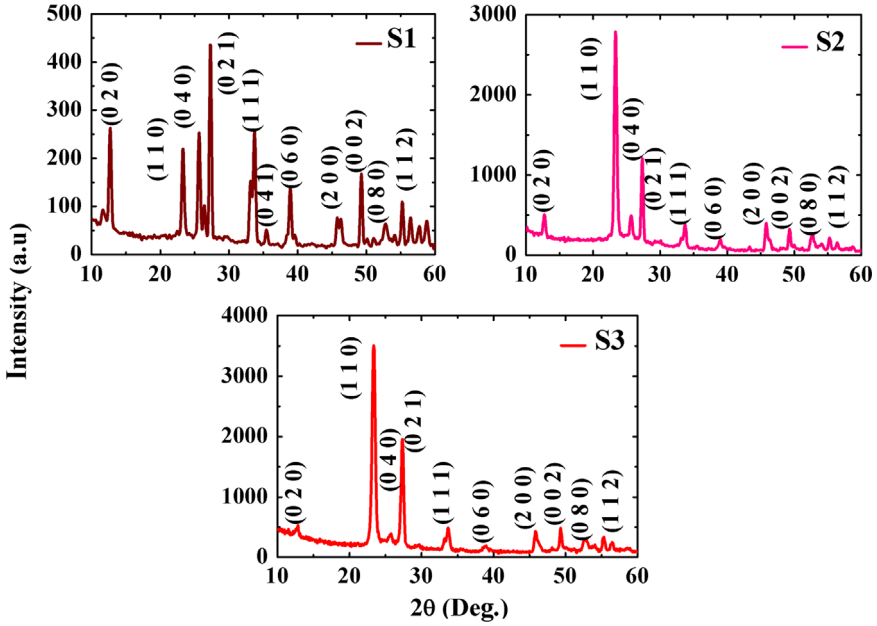

Fig. 1. X-ray diffractograms of MoO_3 nanostructured thin films deposited on: S1–S3.

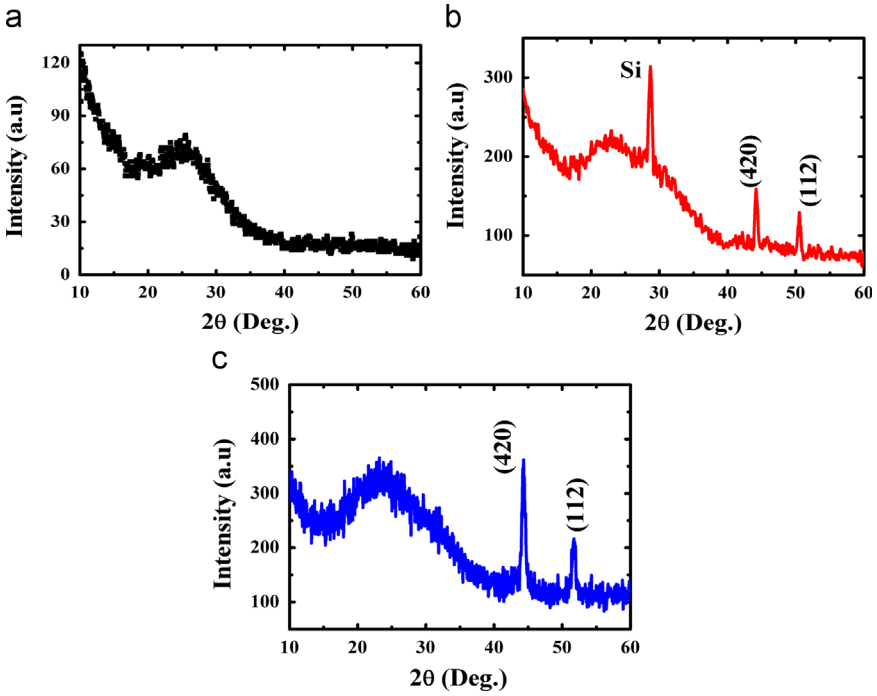

Fig. 2. X-ray diffractrograms of annealed Ni films at 500 °C on (a) ITO/glass, (b) Si [100], and (c) bare glass.

these are precisely consistent to the standard values as reported in the JCPDS file (35-609). In case of sample S1 the intensity of the diffraction peaks obtained from most of crystal planes are significant in terms of intensity. It divulges the randomness in the alignment of grown nanostructures, means no specific preferential growth is taking place in S1. Whereas, the recorded diffraction pattern of MoO_3 thin films particularly in case of S2 and S3 samples shows the substantial increase in the peak intensity corresponding to [110] crystal plane positioned at an angular position 23.4° in compare of other peaks, which strongly evident that nanostructures are growing preferentially along the [110] direction in conjunction of better degree of crystallinity. The estimated mean crystallite size of samples S1, S2, and S3 is found to be 25.5, 33.7, and 40.6 nm, respectively corresponding to the diffraction plane having maximum intensity by using the Debye–Scherrer formula [9]. The relatively larger crystallite size in case of S2 and S3 relative to S1 again assured the betterment in degree of crystallinity and also surmised the dependence of crystallinity and alignment on the employed substrates for deposition. The improved crystallinity as well as alignment in S2 and S3 may be owing to the different average roughness of substrates with Ni/ITO coating and the considerable difference in the thermal expansion coefficients

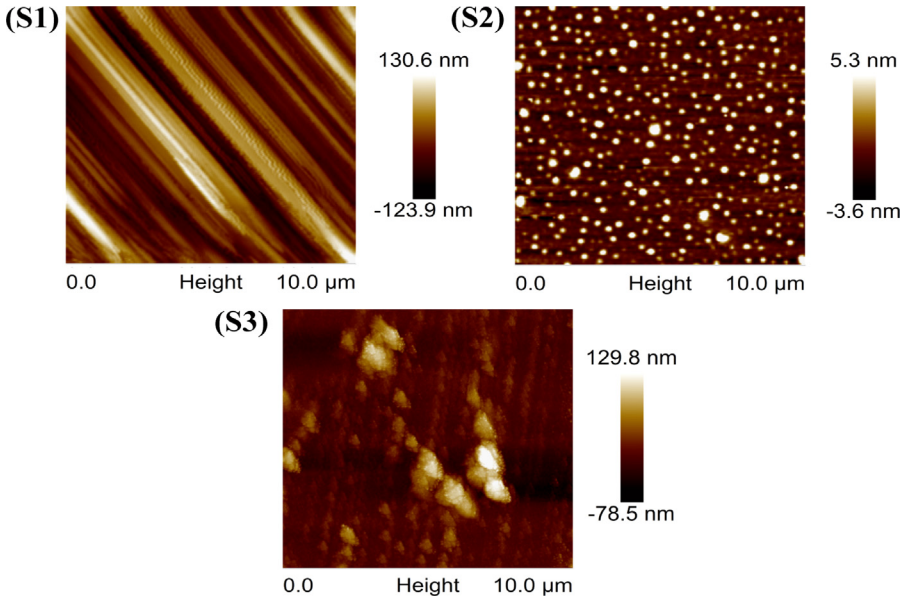

Fig. 3. AFM micrographs of substrates surfaces S1–S3.

between pre-deposited film (Ni/ITO) and the substrates (Si/glass). The presence of less intense XRD peaks corresponding to [420] and [112] planes in case of S2 and S3 evidenced the crystalline nature of nickel films because of microcracking on Ni film at 500 °C (see in Fig. 2b and c). The additional peak appeared in Fig. 2(b) is corresponding to the Si substrate itself. It is to be noted that ITO did not show any peak, indicating its amorphous nature (see in Fig. 2a). The temperature gradient between the upper and lower substrate surfaces is also guiding the incoming MoO_3 molecules to make the growth alignment better in presence of oxygen plasma.

3.2. AFM studies

To investigate the effect of substrate surface roughness on the growth of MoO_3 nanostructures, AFM measurements are performed on all substrates with Ni/ITO films before growth. Fig. 3 shows two dimensional AFM surface images (scale of $10\times 10\ \mu m^2$) of all substrate surfaces. According to AFM analysis, three distinct surface roughnesses are observed and demonstrated in Table 1. The results are confirmed that S2 and S3 have minimum and maximum surface roughnesses, whereas the surface roughness of S1 substrate lies in the intermediate of both. The comparative studies between the observed substrates roughness with Ni or ITO films and the reported average roughness of simple glass and Si substrates divulge that the average roughness of substrates gets enhanced with pre-deposited layer. It is believed that high surface roughness may develop additional micro-strain on pre-deposited layers, when substrate keeping particularly at source temperature 500 °C in oxygen plasma and also affect the number density of micro-cracks existing on pre-deposited films. Roozbehi et al. [18] have been reported that the substrate surface roughness is very crucial and greatly influences the growth of nanostructures. It is conceived that high substrate roughness enhance micro-cracking on pre-deposited layers. The influence of substrate roughness on the features and alignment of grown MoO_3 nanostructures is confirmed by the further characterizations shown in the proceeding sections.

3.3. SEM studies

Fig. 4 shows the SEM micrographs of MoO_3 thin films fabricated on different substrates in oxygen plasma at strip temperature

Table 1
AFM, average surface roughness of all substrates.

Substrates	Average surface roughness (nm)
S1	16.4
S2	1.39
S3	35.8

500 °C revealed the formation of various nanostructures and their dependence on the nature of substrates, whereas Fig. 5 demonstrates the clear view of microcracking taking place on pre-deposited ITO/Ni film on Si and Glass substrates at 500 °C individually. Firstly, the MoO_3 film deposited on ITO/glass substrate (S1) depicts the formation of MoO_3 NP_s of random alignment but distributed nearly in uniform fashion on entire substrate, can be seen in Fig. 4(S1). These NP_s are aligned either in vertical direction or inclined at certain angle relative to substrate without any restriction. Since it has already reported that the developed microcracks on pre-deposited layers is explicitly owing to the significant difference in TEC_s of substrate and pre-deposited layer, which furnish heterogeneous nucleation sites in order to grow vertically aligned nanostructures uniformly [19]. The analysis reveals that almost same thermal expansion coefficient of ITO (9×10^{-6}/K) film and glass (8.5×10^{-6}/K) substrate attributed less strain on ITO film as a result quite less cracking is formed on ITO film, consequently the grown MoO_3 nanostructure could not attain well defined features as well as alignment. The surface morphology in sample S2 endorses the formation of uniformly distributed NP_s on large area scale (see Fig. 4 in S2) assuring that the growth is taking place in uniform fashion on the entire substrate of (20×15) mm^2 area. The film consists of 60 nm thick NP_s (see in inset of S2 in Fig. 4) and most of them are aligned perpendicular to the substrate. The mean height and width of these NP_s are observed to be 1.5 μm and 1 μm, respectively. The cross sectional view of S2 in Fig. 4(S2-C) depicts that NP_s having very high aspect (height/thickness) ratio more than 25. Moreover, the recorded SEM micrograph of sample S3 in Fig. 4(S3) shows the formation of MoO_3 NF_s on Ni/glass substrate with enhanced number density (number of NF_s per unit area) under the same processing parameters in oxygen plasma. Most of the MoO_3 NF_s of thickness 70 nm have the same growth alignment as in case of Ni/Si

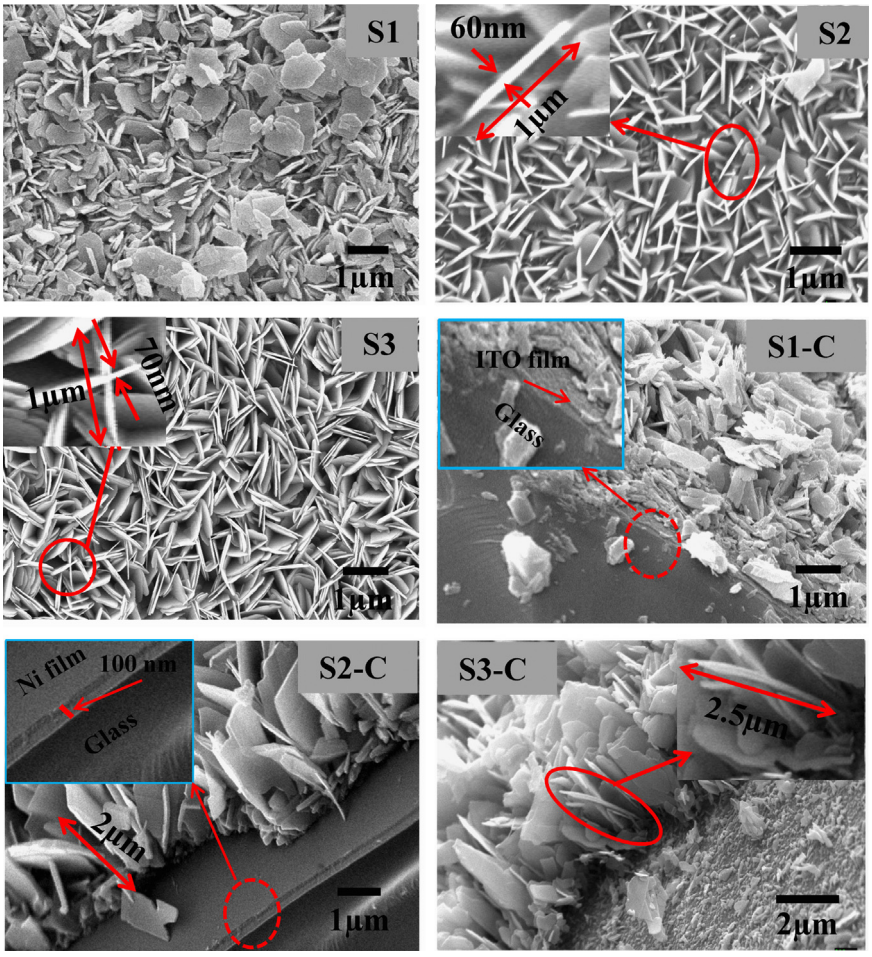

Fig. 4. SEM micrographs of MoO_3 thin films of: S1, S2, and S3 with the corresponding cross-sectional view S1-C, S2-C, and S3-C.

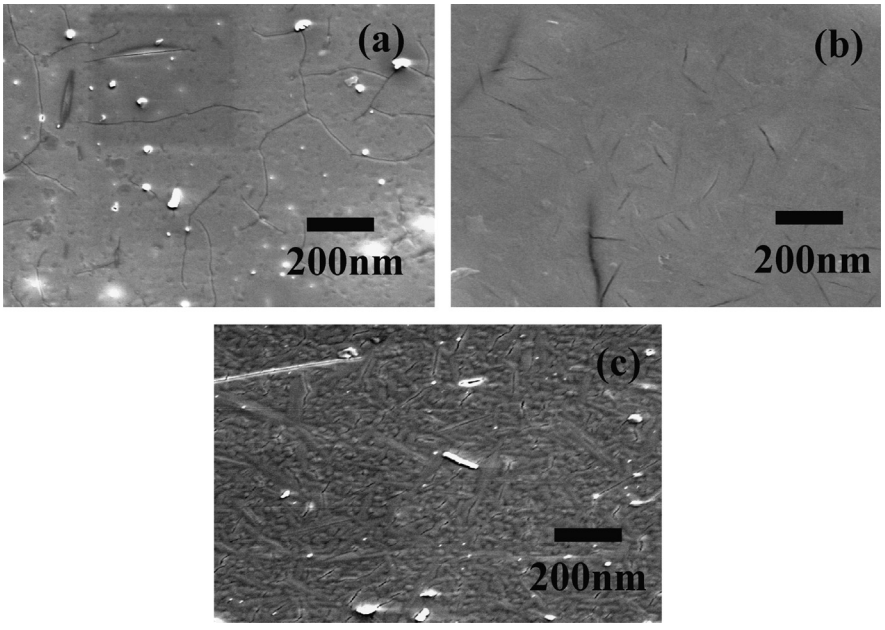

Fig. 5. SEM micrographs of Ni films deposited on (a) ITO/glass, (b) Si [100], and (c) glass substrate.

substrate. The average height and width of nanoflakes are found to be 2.5 μm and 1 μm, respectively. It is worth noting that the aspect ratio of deposited NF_s is >35 relatively more than NP_s grown on Ni/Si substrate (see in S3-C of Fig. 4). It is observed that some flakes are growing parallelly but very close to each other may be due to the Van der Waals interactions. The NF_s those are not

Table 2
Dimensional details of MoO_3 nanostructures grown on various substrates under the same processing parameters.

Type of substrates	Type of nanostructure	Average height (nm)	Average length (nm)	Average thickness (nm)	Aspect ratio (height/thickness)	Crystallite size (nm)
S1	NP_s with improper features	–	–	–	–	35.5
S2	Well aligned nanoplates (NP_s)	2000	900	60	>30	38.3
S3	Vertically aligned nanoflakes (NF_s)	2500	1000	70	>35	40.6

parallel also inclining to fuse into each other as the gap among them reduces owing to the continuous growth. It is also pointed out that after the NF_s conflated together the growth rate along the line of contact get continued as a result multipods like morphology crop out and evidently visualized in the inset of Fig. 4(S3) as well. No restriction could impose either on the number of fused flakes or the angle at which they get attached with others. Table 2 summaries all the dimensional details like average dimensions, aspect ratio, and the crystallite size of all MoO_3 nanostructures grown on different substrates. The possible reason of well aligned and uniform growth in case of both the samples S2 and S3 is the significant gap among the values of thermal expansion coefficients of pre-deposited Ni film (13×10^{-6}/K) and Si (2.7×10^{-6}/K) and glass (8.5×10^{-6}/K) substrates. Because of this difference Ni film and the used substrates are not elongated in the same proportion relatively at the growth temperature 500 °C, result in a strain is develop on Ni film, which produces micro strain/cracking on its surface in oxygen plasma as can be seen in Fig. 5 [20]. In sample S2 the difference in the thermal expansion coefficients of Ni and Si is relatively large, which produce more strain/microcracking on Ni surface (see in Fig. 5b). Besides that, there are three additional factors crystalline nature of Si, high thermal conductivity, and small roughness of Si facilitates to control the feature and alignments of grown nanostructure. According to AFM analysis the surface roughness in S2 is quite small, may not influencing the micro-cracking on Ni film. Therefore the growth in S2 is completely deal by the other factors mentioned above. The experimental outcomes evident that the temperature gradient between the upper and lower surfaces of Ni/Si substrate is trivial because of relatively high thermal conductivity of silicon, which compels the upper surface temperature (where growth is taking place) of sample S2 is relatively higher than others (i.e. S1 and S3). This increased temperature furnish additional thermal energy to migrate the incoming MoO_3 molecules on S2 to attain proper nucleation sites, consequently the well featured and vertically aligned NP_s are formed on S2. The dimensions of NP_s are utterly uniform having no sharp corners. Moreover, the distribution of thermal energy in S2 is relatively uniform on the entire substrate due to its crystalline nature. Hence in sample S2, both the high thermal conductivity and the crystalline nature of silicon substrate are simultaneously monitoring the growth of MoO_3 NP_s on the entire substrate. But in case of sample S3 uniformly distributed MoO_3 NF_s are formed on entire substrate with increased number density than S2. It is reported earlier [19] that microstrain/cracking on pre-deposited films in oxygen plasma at source temperature 500 °C offer the proper seeding for the growth of vertically aligned 2D nanostructures like NP_s and NF_s. It is known that surface roughness profoundly influences strain developed on Ni film. The relatively larger surface roughness in sample S3 might increase the degree of microcracking significantly at temperature 500 °C (see in Fig. 5c). This additional cracking on Ni layer is rendered more nucleation sites on nickel layer, greatly responsible to the enhancement in the number density of NF_s in case of S3 and also agreed with the XRD findings. The value of average surface roughness in Ni/glass is comparable to the diffusion length, so the arriving MoO_3 molecules are not able to migrate properly on substrate due to the high energy barriers for migration and attached with the nearest nucleation site on Ni film, which favors the betterment in the number density of NFs [18]. It is worth noting that although the difference in the thermal expansion coefficients of Ni and amorphous glass is smaller than Ni and silicon. But still the occurrence of vertically aligned NF_s with enhanced number density in S3 affirmed the dominant role of surface roughness on the growth of MoO_3 nanostructures as described above. During growth in S2 and S3 the arriving MoO_3 molecules on substrate are setting on these sharp edges of cracks in the form of long chains during the onset of growth. Once a strong foundation is formed the continuously impinging MoO_3 flux incorporates along the edges of microcracks/strains and strongly recommends the preferential growth along vertical direction. It is to be noticed that the temperature gradient between top and base region will gradually increase with the height of the NP_s/NF_s, preferably favors the vertically aligned growth as well. The larger number density of NF_s and NP_s in sample S2 and S3 is also favorable for better alignment of nanostructures because the dominance of crowding effect [6].

3.4. TEM, HRTEM, and SEAD studies

Sample S2 and S3 are now chosen for further characterization by transmission electron microscopy (TEM) due to the existence of vertically well aligned nanostructures. For TEM measurements, samples are merely dispersed in ethanol along with ultrasonic bath and then scraping the NP_s/NF_s off from the substrate independently and collected these on carbon coated Cu grids. The low magnified bright field TEM micrographs of S2 and S3 are confirming that both the plates and flakes are well formed and possessing very large surface area because of two wide open faces can be seen in Fig. 6(a) and (b). This makes both MoO_3 NP_s and NF_s specific for various technological applications such as Li^+ ion secondary batteries, display devices, and gas sensor devices from the improved efficiency point of view. Further characterizations of S2 and S3 are performed by high resolution electron microscopy (HRTEM) with selected area electron diffraction (SAED) pattern can be seen in Fig. 6(c) and (d), revealed that both NP_s and NF_s are composed of single crystalline orthorhombic α-MoO_3 with top/bottom surface of (010) crystal plane and the growth lying preferentially along the [110] direction. The SAED patterns of individual flake and plate is accompanied with [010] zone axis diffraction revealed in inset of Fig. 6(c) and (d) evidently exhibit diffraction spots, which assigned according to the orthorhombic phase of MoO_3 and strongly evident that the single crystalline plates as well as flakes are growing preferentially along the [110] crystallographic direction. The individually recorded fringe pattern in S2 and S3 from the encircled region with the spacing of 0.381 and 0.378 nm corresponding to (110) planes can easily be detected and very close with the calculated spacing from XRD patterns depicted in Fig. 6(c) and (d). Several NF_s and NP_s are investigated and same results are found.

3.5. Raman analysis

Raman spectroscopy is utilized in order to examine the possible vibrations and symmetry of molybdenum and oxygen atoms in all samples. All the observed Raman peaks positioned at 238, 284,

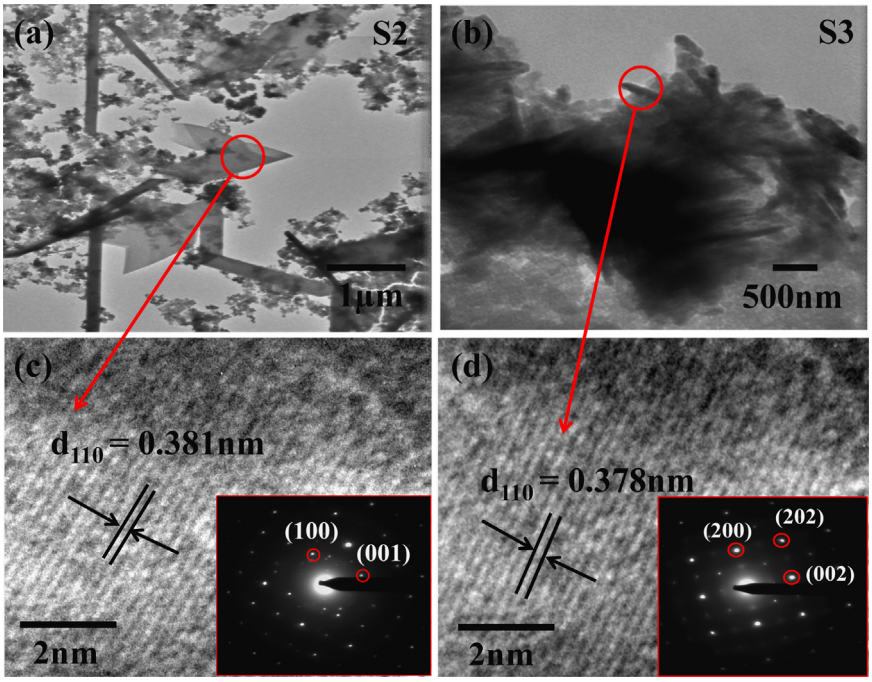

Fig. 6. (a) Bright field TEM images of MoO_3 thin films: (a) S2 and (b) S3 captured at low magnification (c and d) HRTEM image of an individual MoO_3 plate in S2 and flake on S3 recorded from encircled regions with their SAED patterns.

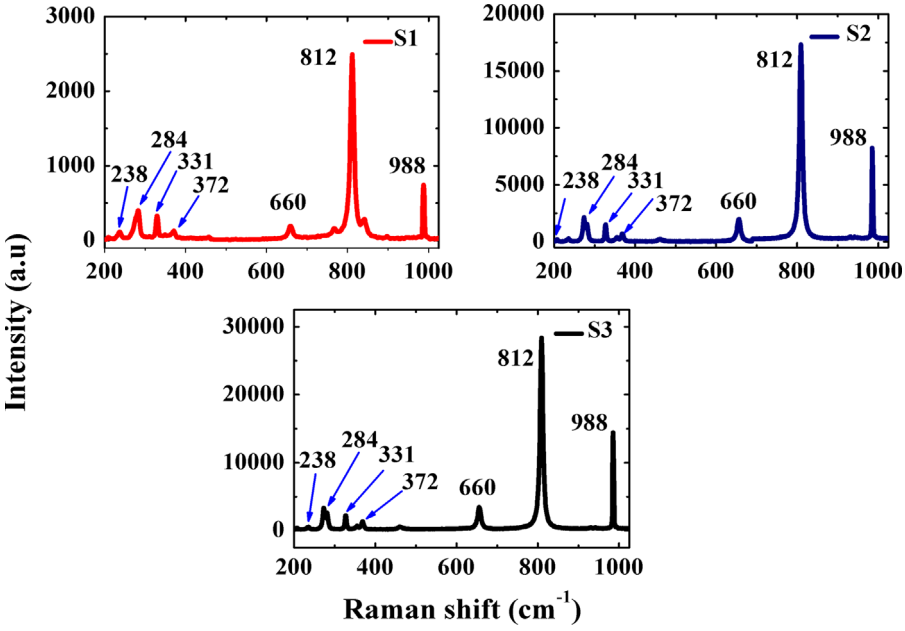

Fig. 7. Micro-Raman spectra of samples S1–S3.

331, 372, 660, 812, and 988 cm^{-1} in all samples are further assured that the grown NP_s/NF_s having only single orthorhombic phase of molybdenum oxide, no peak corresponding to other phase is found [21]. The recorded Raman spectra of samples S1–S3 have sharp peaks with enhanced intensities can be seen systematically in Fig. 7. The relatively higher intensity of peaks in samples S2 and S3 than S1 is the direct consequence of their better degree of crystallinity and in the consonance with XRD outcomes as well. It is reported that the crystalline structure of α-MoO_3 is seldom and can viewed as a corner-sharing chains of MoO_6 octahedra, having one oxygen is unshared, two oxygen atoms are common to two octahedra and three oxygen atoms have partially-shared edges and attach with three independent octahedral units [22]. All these remarkable vibrational peaks mentioned above are evident to the existence of various kinds of Mo–O stretching and bending modes. All the observed Raman peaks are closely resembles the single crystal Raman spectrum as reported by Py and Maschke [23] with the characteristics Raman peaks. The analysis reveal that Raman peaks in all samples display a shift of 4–10 cm^{-1} towards lower wavenumber. This red shifting may be owing to the reduced size of

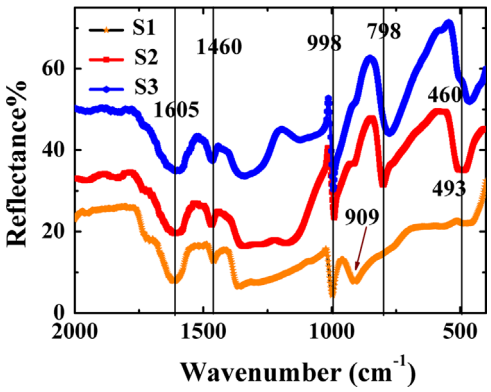

Fig. 8. FTIR spectra of samples S1–S3.

NP_s/NF_s. The sharp intense peak assigned at 988 cm^{-1} corresponds the terminal oxygen (Mo=O) stretching mode, which is the consequence of an unshared oxygen and responsible for the layered structure of α-MoO_3 [24]. The bridging oxygen atoms particularly along the *c*-axis are most loosely bounded resulting in the creation of oxygen/anion vacancies are most probable along the same axis, thus a displacement of Mo-atom towards the terminal oxygen in the *b*-direction can be anticipated with the loss of bridging oxygen, therefore reducing the bond strength of oxygen atom along the *a*-axis [25]. The intense Raman peaks at 812 cm^{-1} is attributed to the mode of stretching of doubly connected oxygen in Mo–O–Mo unit, as a results of corner-shared oxygen common in two octahedral units. The peak around 660 cm^{-1} is assigned to the triply coordinated oxygen (Mo_3–O) stretching mode which results from edge-shared oxygen in common with three octahedra [26]. The low intense Raman peaks positioned along low wavenumber side at 238, 284, 331, and 372 cm^{-1} might be representing to Mo–O_2 scissoring and O=Mo=O wagging modes, respectively [27].

3.6. FTIR analysis

The infrared reflectance spectra of MoO_3 thin films S1–S3 are recorded for the wavenumber scale 400–2000 cm^{-1} further to study the vibrational properties of MoO_3 thin films, shown in Fig. 8. It is revealed from IR spectra that majority of the molecular vibrational frequencies are present in the considered range of wavenumber. The MoO_3 films show seven dominant absorption peaks at 1650, 1460, 998, 909, 798, 493, and 460 cm^{-1}. These observed absorption peaks are attributed to different modes of vibrations. Our study is based on the fact that the MoO_3 is accompanied by distorted MoO_6 octahedra for which stretching and bending IR-active modes are consistently observed in the 450–1000 cm^{-1} region [11]. The relatively more intensity of absorption peaks in samples S2 and S3 endorses the enhancement the dimensions of grown structures owing to the increase in degree of crystallinity as elaborated earlier by Raman and XRD pattern. The existence of stretching mode of oxygen in Mo_2–O unit is clearly specified by the absorption peak located at 909 cm^{-1} whereas the intense peak at 998 cm^{-1} is corresponding to the stretching mode of Mo=O bonding unit and also supports of being its basic characteristic of layered structure particularly in α-MoO_3 [28]. The peak located at 798 cm^{-1} is due to the stretching mode of Mo–O–Mo congruent to the symmetric Mo–O bond length of both the side of oxygen atom. Peak present at 493 cm^{-1} is due to the bending mode of Mo_2–O entity, shifted slightly towards lower wavenumber in sample S3, may be due to the dominance of the Vander wall interaction among NF_s situating in close proximity to each other (can be seen in Fig. 5S3) [29]. The observations obtained from FTIR spectra are completely in agreement with the Raman and XRD results. Two additional intense peaks located at 1605 and 1460 cm^{-1} are corresponding to the bending mode of Mo–OH bond in all films owing to the hydroxylation of film when taking these out of vacuum chamber, assigned the presence of adsorbed free water molecules [29].

4. Conclusions

In summary, we demonstrated the influence of substrate effect on the growth of MoO_3 nanostructures fabricated by plasma assisted sublimation process (PASP). Three different substrates viz. ITO/glass, Ni/Si [100], and Ni/glass are used in this work. The AFM results reveal that the degree of substrate roughness is greatly affect the growth of nanostructures on substrates. The structural and morphological results endorse that the Ni/glass substrate are relatively more favorable for the uniform growth of MoO_3 NF_s with the highest aspect ratio (height/thickness) > 35 on large area scale, whereas vertically aligned MoO_3 NP_s are grown on Ni/Si [100] substrate with slightly lesser aspect ratio (~30) than NF_s. But in case of ITO coated glass NP_s are formed with improper features. The grown nanostructures on various substrates are polycrystalline in nature having pure orthorhombic phase, no impurity is observed. HRTEM analysis with SAED assured that both the MoO_3 NP_s and NF_s are single crystalline in nature and growing preferentially along the [100] direction. The vibrational study of all films are carried out by micro-Raman and infra-red (IR) spectroscopy, assured that the size and growth of nanostructures greatly influenced the vibrational properties of material. These novel nanostructures fabricated by plasma assisted sublimation process (PASP) might offer great opportunities for both the fundamental research and technological applications.

Acknowledgment

One of the authors Rabindar K. Sharma gratefully acknowledges the financial assistance from Council of scientific and industrial research (CSIR)-India.

References

[1] A. Singh, S. Chaudhary, D.K. Pandya, Appl. Phys. Lett. 102 (2013) 172106.
[2] J.N. Yao, K. Hashimoto, A. Fujishima, Nature 355 (1992) 624.
[3] Tarsame S. Sian, G.B. Reddy, J. Appl. Phys. 98 (2005) 026104.
[4] M.B. Rahmania, S.H. Keshmiri, J. Yua, A.Z. Sadek, L. Al-Mashat, A. Moafi, K. Latham, Y.X. Li, W. Wlodarski, K. Kalantar-zadeh, Sens. Actuators B 145 (2010) 13.
[5] Damien P. Debecker, Mariana Stoyanova, U.W.E. Rodemerck, Eric M. Gaigneaux, J. Mol. Catal. A: Chem. 340 (2011) 65.
[6] Can Liu, Zhengcao Li, Zhengjun Zhang, Appl. Phys. Lett. 99 (2011) 223104.
[7] Yixin Sun, Jie Wang, Bote Zhao, Rui Cai, Ran Ran, Zongping Shao, J. Mater. Chem. A 1 (2013) 4736.
[8] L.Q. Mai, B. Hu, W. Chen, Y.Y. Qi, C.S. Lao, R.S. Yang, Y. Dai, Z.L. Wang, Adv. Mater. 19 (2007) 3712.
[9] T. Siciliano, A. Tepore, E. Filippo, G. Micocci, M. Tepore, Mater. Chem. Phys. 114 (2009) 687.
[10] Lili Cai, Pratap M. Rao, Xiaolin Zheng, Nano Lett. 11 (2011) 872.
[11] K. Srinivasa Rao, B. Rajini Kanth, P.K. Mukhopadhyay, Appl. Phys. A 96 (2009) 985.
[12] A.K. Prasad, D.J. Kubinski, P.I. Gouma, Sens. Actuators B 93 (2003) 25.
[13] Jun Zhou, S.Z. Deng, N.S. Xu, Jun Chen, J.C. She, Appl. Phys. Lett. 83 (2003) 2653.
[14] C.-S. Hsu, C.-C. Chan, H.-T. Huang, C.-H. Peng, W.-C. Hsu, Thin Solid Films 516 (2008) 4839.
[15] B. Yan, Z. Zheng, J. Zhang, H. Gong, Z. Shen, W. Huang, T. Yu, J. Phys. Chem. C 113 (2009) 20259.
[16] A. Khademi, R. Azimirad, A. Asghar Zavarian, A.Z. Moshfegh, J. Phys. Chem. C 113 (2009) 19298.
[17] E. Comini, L. Yubao, Y. Brando, G. Sberveglieri, Chem. Phys. Lett. 407 (2005) 368–371.
[18] Maryam Roozbehi, Parvaneh Sangpour, Ali Khademi, Alireza Z. Moshfegh, Appl. Surf. Sci. 257 (2011) 329.
[19] Rabindar K. Sharma, G.B. Reddy, J. Appl. Phys. 114 (2013) 184310.
[20] Rabindar K. Sharma, G.B. Reddy, AIP Adv. 3 (2013) 092112.

[21] M. Dieterle, G. Mestl, Phys. Chem. Chem. Phys. 4 (2002) 822.
[22] G. Andersson, A. Magneli, Acta Chem. Scand. 4 (1969) 793.
[23] M.A. Py, Ph.E. Schmid, J.T. Vallin, Nuovo Cimento 271 (1977) 38B.
[24] I.R. Beattie, T.R. Gilson, J. Chem. Soc. A (1969) 2322.
[25] G. Mestl, N.F.D. Verbruggen, E. Bosch, H. Knozinger, Langmuir 12 (1996) 2961.
[26] G.M. Ramans, J.V. Gabrusenoks, A.R. Lusis, A.A. Patmalnieks, J. Non-Cryst. Solids 90 (1987) 637.
[27] M.A. Py, K. Maschke, Physica B 105 (1981) 376.
[28] M. Anwar, C.A. Hogarth, C.R. Theocharis, J. Mater. Sci. 24 (1989) 2387.
[29] T.S. Sain, G.B. Reddy, Appl. Surf. Sci. 236 (2004) 1.